Lançadores Espaciais[☆] (1st year, MEAer)

Academic Year 2024/25

Gravity-Turn With Atmosphere

Rodrigo Pereira (112117), David Ribeiro (112202), Alexandre Pereira (112288), Alessandro Melifiori (112400), Marta Pellegrino (112399), João Almeida (103026), Joshua Redelbach (112470)[*]

Abstract

This report discusses the optimization of the kick angle during a gravity turn maneuver for a two stage rocket orbital injection, aiming to minimize the total amount of needed propellant. Losses due to gravity and aerodynamic drag are considered. The mission profile analyzed includes vertical lift-off, gravity turn maneuver, coasting phase and orbit injection. Two approaches for orbit injection into a circular orbit are analyzed: single burn and double burn. Results of the developed software are provided and compared to a real case scenario.

Keywords: gravity-turn, space launch, optimization, ascent trajectory

Contents

[☆]Space Launchers.

[*]Team #4
Email address: joshua.redelbach@tecnico.ulisboa.pt (Joshua Redelbach (112470))

1. Introduction

When a rocket is launched, the first few moments after lift-off are characterized by a vertical flight path to ensure the launcher experiences the lowest aerodynamic drag possible [1]. In order to insert the rocket into the correct orbit [1], when the atmospheric density becomes adequately low [2], a turning maneuver to tilt the velocity vector towards the horizon is performed [2].
This crucial maneuver can be performed employing the gravitational force of the Earth, through the so-called "Gravity Turn" [2]. The advantage of using this technique lies in saving the propellant that would be needed to steer the rocket [1], exploiting the natural tendency of a body in a parabolic motion to reach a null vertical velocity component at the highest point of the trajectory [1].
Since the gravity turn maneuver requires the rocket not to lie on a vertical flight path, a pitch maneuver is first performed to give the launcher an initial kick angle [1]; only after acquiring it, the pitch angle can then increase up to the desired value [1].
The goal of this project is to optimize the aforementioned kick angle for a two-stage rocket to get into a desired final circular orbit by minimizing the required propellant. For this, two different possible solutions for orbit injection and circularization are investigated in order to determine which method requires the lowest propellant consumption. For this purpose, a detailed simulation is developed. Other values, such as altitude, velocity and flight path angle will be evaluated as a function of time.

2. Theoretical Fundamentals

2.1. Equations of Motion

In order to discuss the motion of the rocket, the following quantities need to be defined first (Fig. 1):

- $\boldsymbol{L}$ = Lift
- $\boldsymbol{D}$ = Drag
- $\boldsymbol{F}_*$ = Thrust
- $\boldsymbol{G}$ = Gravitational Force
- $\boldsymbol{v}$ = Velocity
- α = Steering Angle (angle between velocity and thrust vectors)
- γ = Flight Path Angle (angle between local horizon and velocity vector)
- $\mathbf{r}$ = distance from Earth's center

It is possible to write down the equation of motion for the rocket during its ascent in its vectorial form [1]:

$$m\frac{d\dot{\boldsymbol{r}}}{dt} = \boldsymbol{F_*}(t) + m\boldsymbol{g}(\boldsymbol{r}) + \boldsymbol{D}(\boldsymbol{v},\boldsymbol{r}) + \boldsymbol{L}(\boldsymbol{v},\boldsymbol{r}) \tag{1}$$

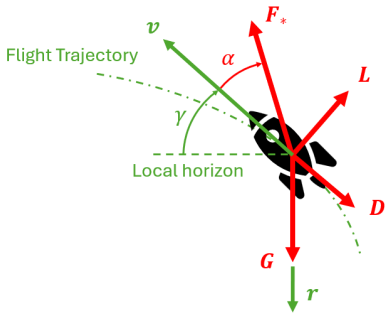

Figure 1: Dynamics Diagram of a Rocket (Based on [1])

In this work, all forces and motions are assumed to lie in a 2D plane. Therefore, in a 2D reference frame, this equation splits in two scalar ones, the first showing the time variation of the velocity v and the second the time variation of the flight path angle γ [1]:

$$\begin{cases} \dot{v} = \frac{F_*}{m}\cos\alpha - \frac{D}{m} - g\sin\gamma \\ v\dot{\gamma} = \frac{F_*}{m}\sin\alpha + \frac{L}{m} - \left(g - \frac{v^2}{r}\right)\cos\gamma \end{cases} \tag{2}$$

where m is the mass of the rocket at time t. It is also possible to extract the time variation of the distance to Earth center r and the downtrack s as follows [1]:

$$\begin{cases} \dot{r} = v\sin\gamma \\ \dot{s} = \frac{r_{earth}}{r} v\cos\gamma \end{cases} \tag{3}$$

However, velocity and position are expressed with respect to the ECI reference frame [3]. Therefore, the conversion is given by:

$$\begin{cases} \theta = \frac{s}{r_{earth}} \\ x = \frac{h+r_{earth}}{sin(\theta)} \\ y = \frac{h+r_{earth}}{cos(\theta)} \end{cases} \tag{4}$$

where θ is the true anomaly, x the component of the coordinate system with respect to the vernal equinox axis, y the component of the coordinate system regarding the axis which is perpendicular to the x one, pointing to the longitude east of the vernal equinox [4] and $r_{earth} = 6378\,\text{km}$ is the radius of Earth. Following, s the down-range relative to non-rotating planet (Earth in this case) and h the altitude over mean sea level.

One important aspect that has to be mentioned is that the presented equations of motion do not model the influence of the Earth's rotation. During launch depending on the location of the launch site and of the departure heading angle, the rocket has an initial velocity due to the Earth's rotation. For simplification purposes of this work, this effect is neglected and the above presented equations of motion are used.

2.2. Mass Flow Rate

The propulsion principle of a rocket is based on action-reaction where some particles are continuously exhausted pushing the vehicle into the opposite direction, while decreasing the mass and increasing linear velocity. However, this continuous mass ejection stream produces a gain in the rocket speed. The evolution of the mass of the rocket with time is known as mass flow rate, $\dot{m}$, and determined by [1]:

$$I_{sp} = \frac{v_*}{g_0} = \frac{F_*}{\dot{m}_p g_0} \Rightarrow \dot{m}_p = \frac{F_*}{I_{sp} g_0} \Rightarrow \dot{m} = -\frac{F_*}{I_{sp} g_0} \tag{5}$$

where F_* is the total trust force, I_{sp} the specific impulse and g_0 is Earth's mean gravitational acceleration on its surface.

2.3. Gravity Turn Principle

During and immediately after lift-off, the launcher is in a vertical position, with $\gamma = 90°$, $\alpha = 0°$, $L = 0$ and $D = 0$ [1]. By substituting these values into the Eq. 2 for the flight path angle rate [1]:

$$\dot{\gamma} = -(\frac{g}{v} - \frac{v}{r})cos\gamma \tag{6}$$

it is evident that $\dot{\gamma} = 0$ for the first phases of the flight, meaning that the launcher will follow a vertical trajectory. In practice, an initial small yaw maneuver is performed to move away from the launch tower, however it is not considered in the project.

To start the gravity turn at a given altitude, a pitch program is used to give the rocket an initial kick angle ($\alpha \neq 0°$), deviating from the vertical direction ($\gamma \neq 90°$) [1]. Thus, based on Eq. 6, the flight path angle will begin to decrease, starting the gravity turn maneuver. From then on, the rocket keeps again $\alpha = 0°$ so that the direction of the following trajectory is only influenced by the gravity force, as lift can be neglected [1]. A "pure" gravity turn usually ends by shutting down the engine when $\gamma = 0°$ is reached, meaning the rocket flies horizontally with respect to Earth.

2.4. Constraints of Gravity Turn

It is important to mention, that only a variation of the initial kick angle α is not sufficient to get into a circular orbit with a certain desired altitude by performing a "pure" gravity turn. This is because for a given engine and its provided thrust, the velocity with which the rocket reaches $\gamma = 0°$ is fixed. This means that, if the engine is shut down at this point, the resulting orbit will not necessarily circular. This gets clear, when looking again at Eq. 6 for this case. To stay on a circular orbit, the flight path angle has to stay constantly 0°, meaning the flight path rate needs to stay zero:

$$\dot{\gamma} = -(\frac{g}{v} - \frac{v}{r_{circ}})cos\gamma \Rightarrow 0 = -(\frac{g}{v} - \frac{v}{r_{circ}}) \tag{7}$$

This equation is only true, if the velocity v with which the rocket reaches $\gamma = 0°$ at r_{circ} is equal to the orbit velocity v_{circ} of the desired circular orbit r_{circ}. If that is not the case, the flight path angle changes, meaning the rocket is on an elliptical orbit. In fact, there is only one circular orbit that can be reached by a certain rocket when performing a "pure" gravity turn.

2.5. Trajectory Types

To reach a desired orbit by using the main principle of a gravity turn, two approaches are analyzed in this work. A summary of the different phases of those two approaches, as well as the "pure" gravity turn, is presented in Tab. 1.

<table>
<tr><th>Phases</th><th>Pure Gravity Turn</th><th>CSB</th><th>CDB</th></tr>
<tr><td>1.</td><td colspan="3">Vertical lift off $\gamma = 90°$</td></tr>
<tr><td>2.</td><td colspan="3">Pitch maneuver with certain α</td></tr>
<tr><td>3.</td><td colspan="3">Gravity turn (thrust with $\alpha = 0°$)</td></tr>
<tr><td>4.</td><td colspan="3">Stage separation</td></tr>
<tr><td>5.</td><td rowspan="5">Gravity turn until $\gamma = 0°$ $\rightarrow$ engine shutdown</td><td colspan="2">Gravity turn until t_{coast}</td></tr>
<tr><td>6.</td><td colspan="2">Coasting until apogee $\gamma = 0°$</td></tr>
<tr><td>7.</td><td rowspan="3">Δv to circularize</td><td>Δv_1 to transfer orbit</td></tr>
<tr><td>8.</td><td>Coasting until transfer apogee</td></tr>
<tr><td>9.</td><td>Δv_2 to circularize</td></tr>
</table>

Table 1: Summary of the phases of the different approaches: pure gravity turn, Coasting Single Burn (CSB) and Coasting Double Burn (CDB).

2.5.1. Coasting Single Burn

The first approach, the Coasting Single Burn (CSB) method, performs a pure gravity turn up to a certain altitude at which the atmospheric effect on the rocket can be neglected and the first stage is already burnt and separated. Then, the second stage shuts down the engine after a certain time and the rocket coasts until it reaches the apogee ($\gamma = 0°$) of the current trajectory around Earth. Based on the initial kick angle α, the time to stop the second stage engine and start coasting, t_{coast}, needs to be optimized so that the apogee is equal to the radius of the desired circular orbit ($r_{apogee} = r_{circ}$). When the rocket reaches the apogee with a certain velocity v_{apogee}, a $\Delta v = v_{circ} - v_{apogee}$ is applied by igniting the engine again to circularize the orbit. Depending on the choice of the initial kick angle α, the propellant consumption of the second engine differs, as the time to start coasting (t_{coast}) and the Δv change. Thus, to get the most propellant-efficient CSB launch, α must be optimized.

2.5.2. Coasting Double Burn

The second approach, the Coasting Double Burn (CDB) method, differs only in the last phases from the CSB launch. After performing a gravity turn, separating successfully the first stage and reaching an altitude at which the atmospheric effect on the rocket can be neglected, the rocket starts coasting after a certain time t_{coast} until it reaches the apogee ($\gamma = 0°$) of the current trajectory. However, in CDB, this apogee r_{apogee} has to be lower than r_{circ}. Then, the rocket performs a Δv_1, to get onto a transfer orbit whose apogee is equal to the desired orbit radius r_{circ}. Reaching this apogee of the transfer orbit, the rocket performs another Δv_2 to circularize the orbit (apogee boost). This approach is similar to a Hohmann transfer.

To find the most propellant-efficient way of performing a CDB launch, the initial kick angle α as well as the time to start coasting t_{coast} needs to be optimized, since they influence

the required total $\Delta v = \Delta v_1 + \Delta v_2$ and thus the required propellant for the two burns, as well as the propellant burnt until coasting.

2.6. Environmental Models

As seen in the equations above, the trajectory is not only influenced by the thrust and the steering angle of the rocket, but also by forces which occur due to gravity and the atmosphere. In the following subsections, models used to mimic their impact are presented.

2.6.1. Gravity Model

Gravity decreases with distance from the center of the Earth. Although this variation is small, it must be considered in the design of a space mission and can be computed with [1]:

$$g(r) = g_0 \frac{r_{earth}^2}{r^2} = \frac{\mu}{r^2} \tag{8}$$

where r is the distance from the rocket to the Earth's center and μ the standard gravitational parameter which is $3.986004418 \cdot 10^{14}\ \mathrm{m^3/s^2}$ in the case of the Earth.

2.6.2. Atmosphere Model

The Earth's atmosphere significantly influences the trajectory of a rocket during its ascent. However, modeling the atmosphere isn't trivial. One approximation for the density, that is often used for simulation purposes, is the exponential law [1]:

$$\rho = \rho_0 e^{-\frac{h}{H}} \tag{9}$$

where ρ_0 is the density at mean sea level ($1.225\,\mathrm{kg/m^3}$), h is the altitude of the rocket with respect to mean sea level and $H = T_0 R / g_0 \approx 6700\,\mathrm{m/K}$, the scale height. Although the rocket will reach altitudes where the density model is not correct, the exponential approximation can be done, since the impact of the atmospheric density on the rocket can be, in general, greatly diminished after reaching an altitude of 65 km [2].

2.6.3. Drag Model

Air exerts a force on the rocket that is opposite to the velocity vector and therefore introduces losses that must be taken into account. This force is referred to as drag and can be approximately described by [1]:

$$D = \frac{1}{2} \rho v^2 C_D A \tag{10}$$

where v is the velocity of the rocket, C_D the drag coefficient, which includes both pressure and friction effects, and A the cross-sectional area of the rocket. It is important to emphasize that this force is not constant, since not only density but also the drag coefficient depend on altitude. However, as an approximation for the simulation of this project, C_D is assumed to be constant.

2.6.4. Lift Model

Air also produces a force, perpendicular to the velocity vector, in case there is a steering angle ($\alpha \neq 0$), that will deviate the rocket from its trajectory. This force is known as lift [1]:

$$L = \frac{1}{2}\rho v^2 C_L A \tag{11}$$

However, during all phases of the ascent trajectory of this work, except for the pitch maneuver, the steering angle α is considered to be zero. Furthermore, the rocket is assumed to be symmetric along the longitudinal axis, allowing lift to be considered negligible.

2.7. Ascent Trajectory Losses

As it was introduced in the previous section 2.6, during the ascent phase of a space launcher, various losses reduce the efficiency of the trajectory and increase the required velocity to reach orbit. These losses are crucial indicators of trajectory performance, as they determine the total Δv budget needed for a successful launch. The main losses include gravity losses, aerodynamic (drag) losses, and steering losses. However, the latter can be neglected due to $\alpha = 0$ in most phases of a gravity turn [5]. The losses are usually analyzed during the powered ascent [5], meaning, for the scenarios in this work, until the second stage stops burning and the coasting begins.

2.7.1. Gravity Losses

Gravity losses occur because the rocket must continuously counteract Earth's gravitational pull while ascending. The longer the rocket spends fighting gravity, the more velocity is lost. Gravity losses are given by:

$$\Delta v_{\text{gravity}} = \int_0^{t_{end}} g(t) \sin\gamma(t)\ dt \tag{12}$$

where g is the local gravitational acceleration, γ is the flight path angle, and t_{end} is time until the loss is to be analyzed. To minimize gravity losses, launch trajectories aim for an early pitch-over maneuver to reduce the time spent in a near-vertical ascent [5].

2.7.2. Drag Losses

Drag losses result from the aerodynamic resistance exerted by the atmosphere on the rocket. These losses are most significant in the lower atmosphere and can be expressed as:

$$\Delta v_{\text{drag}} = \int_0^{t_{end}} \frac{C_D A \rho(t) v(t)^2}{2m(t)}\ dt = \int_0^{t_{end}} \frac{D(t)}{m(t)}\ dt \tag{13}$$

where C_D is the drag coefficient, A is the reference area, ρ is the atmospheric density, v is the velocity, m is the mass of the rocket and and t_{end} is time until the loss is to be analyzed. To reduce drag losses, rockets typically ascend quickly through the denser atmospheric layers and use streamlined designs to minimize aerodynamic resistance [5].

2.8. Dynamic Pressure

The equation of dynamic pressure, $q = \frac{1}{2}\rho v^2$, can be easily derived from a one-dimensional version of the conservation of linear momentum for a fluid.

"The dynamic pressure depends on both the local value of the density and the velocity of the flow, or rocket. The density of the air decreases with altitude in a complex manner. The velocity of a rocket during launch is constantly increasing with altitude. [...] The dynamic pressure increases because of the increasing velocity to some maximum value, called the maximum dynamic pressure, or Max Q. Then the dynamic pressure decreases because of the decreasing density." [6]

With the Eq. 9 from the density model and velocity and altitude information provided by SpaceX's live-streams on YouTube, [7], it was possible to calculate the Max Q experienced by Falcon 9 in various missions. A large sample of videos suggests that typical values of Max Q for Falcon 9 missions can range between 14 kPa [8] and 23 kPa [9]

3. Simulation

For the analysis of the two launch approaches, CSB and CDB, a simulation was developed in *python*. In the following chapter, its design and implementation are presented. First, it is explained how the ascent trajectory is implemented and what user-specific parameters can be set. Then, the optimization algorithms for CSB and CDB are presented. Lastly, a summary is given of what the simulation provides as output for the user. A block diagram of the general architecture of the simulation software is given in the Appendix B in Fig. B.7.

3.1. Ascent Trajectory

In general, the rocket dynamics are implemented as presented in Sec. 2.1. They are integrated over time using the Runge-Kutta 5 algorithm. The time steps for this integration can be specified by the user. The models for gravity, atmosphere and drag are implemented as introduced in Sec. 2.6. The user can set the properties of both stages, including the wet and dry mass as well as the engine parameters (specific impulse I_{sp} and thrust F_*) and also the cross section area A or the drag coefficient C_D of the rocket. In the simulation, it is assumed that the rocket only consists of the structure and propellant mass of the two stages and not any additional payload mass. The amount of payload that can be carried is later calculated by determining the mass of propellant left on the second stage. In the following, it is explained how the different phases (see Tab. 1) are implemented.

The vertical lift off is simulated by initializing the rocket state:

$$[s, r, v, \gamma, m] = \left[0\,\mathrm{m}, r_{earth}, 10\,\mathrm{m\,s^{-1}}, 90°, m_{initial}\right] \tag{14}$$

and simply keeping the steering angle $\alpha = 0°$. This leads to no change in the flight path angle γ and thus to vertical ascent.

The pitch maneuver starts after reaching a time stamp that can be set by the user. Then, the steering angle α is linearly increased up to a maximum value α_{max} and subsequently linearly decreased until $\alpha = 0°$. The duration of this maneuver is also specified by the user. The value of α_{max} is found by the optimization.

Next, the gravity turn is simulated until the propellant of the first stage is burnt. To simulate a realistic stage separation phase, a delay between first engine shutdown and cutoff, as well as between first engine cutoff and second engine ignition, is simulated. This is done by simply applying no thrust in the two periods. The duration of the delays can be set by the user. The separation of the stages is simulated by assuming instantaneous loss of the first stage with no impulsive effects on the second stage.

Afterwards, the gravity turn is simulated until the coasting begins, meaning setting the thrust to zero. This timestamp is found by the optimization. As the optimization makes sure that the coasting phase only starts when the rocket is high enough to neglect atmospheric effects, the simulation continues by setting the drag D to zero. This coasting phase goes until the apogee is reached, meaning $\gamma = 0°$.

When the CSB approach is simulated, reaching the apogee means reaching the altitude of the desired orbit. Thus, a Δv is applied to circularize the orbit. This maneuver is assumed to be instantaneous. Therefore, in the simulation, the Δv is added to the current velocity state v. This idealization is only valid when the position of the rocket changes only slightly during the time that the engine fires. This is true for rockets with burn times that are very short compared to the orbital period [10]. So that the simulation can use this realistic assumption, the burn time required for that Δv needs to be constrained to $t_{burn,max}$. To enable a realistic simulation, the maximum burn time of the maneuver shall be less than $t_{burn,max} = 15$ s.

When simulating the CDB approach, after reaching the apogee, a first Δv_1 is applied in the same way as in the CSB approach. Then, another coasting phase is simulated until reaching the apogee of the transfer orbit that has the same altitude as the desired orbit. Thus, a second Δv_2 is applied to circularize the orbit. The constraint on the burn time for both Δv is the same as for the CSB maneuver.

3.2. Optimization

Two optimization algorithms were developed, one for the CSB and one for the CDB ascent approach. Flow charts describing their procedure are depicted in Fig. 2. The goal of both algorithms is to minimize the total propellant required to get into a desired circular orbit by optimizing the maximum steering angle α, also referred to as angle of attack, in the pitch maneuver. This way, the amount of payload that can be carried to orbit can be maximized by assuming all the propellant mass that is left of the second stage could have been payload mass at launch. The altitude of the desired orbit can be specified by the user. Therefore, the general procedure for both approaches is the same. A cost function returns the total propellant required by the second stage, given an angle of attack. Then, using an optimizer like differential evolution and a given range for the angle of attack, the optimal angle that minimizes the cost function is found. However, the implementation of the cost function is different for the two approaches.

For the CSB approach, the ascent trajectory is simulated until the rocket reaches an altitude at which atmospheric effects can be neglected. This is the case at 65 km [2]. At this time, the first stage is already burnt and separated. Then, the apogee is calculated if the orbit that would result if the engine were to stop burning at that moment and the

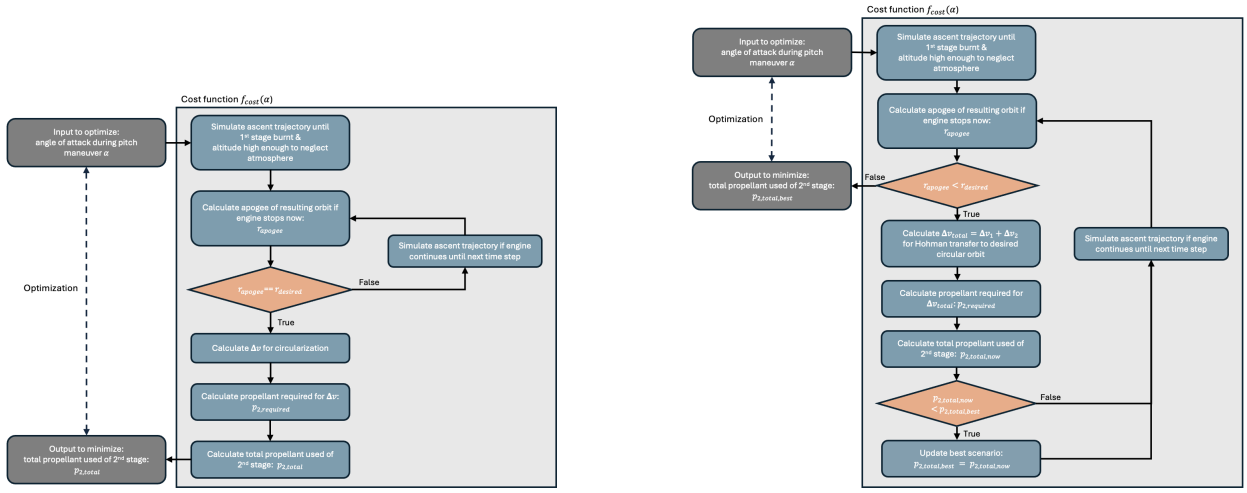

(a) CSB (b) CDB

Figure 2: Flow charts for the optimization algorithms used for the single (CSB) and double burn (CDB) simulations.

atmospheric effects were neglected. If this apogee is equal, up to a certain margin of $0.2\% \cdot (h_{desired} + r_{earth})$ of the desired orbit radius, the time to start coasting, t_{coast}, is found and the Δv for circularizing the orbit is calculated. Based on this value, the total propellant used by the second stage is determined and returned as the cost for this angle of attack α. If the apogee is not equal to the desired orbit radius, the ascent trajectory is simulated until the next time step and the procedure repeats. If no scenario in which the rocket reaches the desired altitude exists for the given angle of attack, an unrealistically high cost is returned to make sure that this case will not be selected by the optimizer.

The difference of the CDB compared to the CSB approach is that for a given angle of attack α, there is not only one time to start coasting t_{coast} so that the desired orbit can be reached, but infinitely many, since the rocket could, in theory, just perform a Hohmann transfer from any altitude. Therefore, first, for a given α that minimizes the propellant used, the optimal time to start coasting, t_{coast}, has to be found. This is done by trying all possible t_{coast} as long as the resulting apogee of the first coasting phase is smaller than the desired orbit radius. For each scenario, the required Δv_{total} for the Hohmann transfer is calculated, as well as the resulting total propellant used. The scenario with minimal propellant used is then returned as the cost for the given angle of attack α.

For both procedures, the cost of scenarios where the required burn time of a single Δv burn exceeds $t_{burn,max}$ is set to unrealistically high values to circumvent them. The simulation implements two possible optimizers for finding the angle of attack that minimizes the required propellant: differential evolution and brute-force. As some scenarios have to be manually set to a high cost, the cost function is not smooth, which can cause difficulties for the differential evolution to converge. Therefore, a brute-force can be used in these cases. In summary, the user can specify the desired altitude, the type of ascent approach to be optimized (CSB or CDB), a range for α and the optimizer to be applied (differential

evolution or brute-force).

3.3. Output

After running the simulation, several data is provided to analyze the final, optimal trajectory. Plots are created that show the rocket's state (downtrack, altitude, velocity norm, flight path angle and mass), the dynamic pressure, the steering angle and the losses (gravity, drag and total loss) over time. Additionally, in the terminal, values are provided indicating an overview of the propellant, the optimal angle of attack, the optimal altitude and time to start coasting and the amount of Δv of the maneuvers, as well as the final orbital elements, final losses, Max Q and burn times for all Δv. Furthermore, a visualization of the trajectory is created showing the orbit around Earth.

4. Evaluation

In the following chapter, the analysis procedure, the used parameters, the results as well as their discussion are presented.

4.1. Analysis Procedure

To compare the two ascent approaches, the results of the optimization are evaluated using a realistic scenario. This consists of using the model of the Falcon 9 rocket launching into a desired low Earth orbit with 500 km so that a comparison of the possible payload can be done. Further, two other higher desired orbits are tested to analyze their impact on the approaches: 2000 km and 20 000 km. Additionally, the feasibility of the resulting trajectory is checked regarding the maximum dynamic pressure. Lastly, the losses are discussed and evaluated.

4.2. Parameters

4.2.1. Vehicle Model

This subsection contains an overview of some parameters of existing rockets that will be used to develop the simulation model. SpaceX's Falcon 9 was chosen for the simulation.

Firstly, it's essential to gather information on the details of the pitch maneuver, namely the time at which the initial kick is executed. Falcon 9's user guide [11] states that an initial pitch maneuver occurs 7.5 seconds after liftoff, with the gravity turn beginning at 55 seconds, followed by max-Q just 21 seconds later. This suggests a duration of 47.5 s for the pitch maneuver.

At T+158s, the first-stage engines are shut down. There is a 3 s delay until the first engine is cutoff (MECO) and an additional 8 s delay between first engine cutoff and second engine ignition [12].

Another important parameter to consider is the drag coefficient. As it was not possible to find an exact value for the C_D of Falcon 9, it was necessary to use an estimation based on other rockets. Based on [13], which gives insights about the drag coefficient of the Saturn V rocket, a value of $C_D = 0.3$ was chosen.

Finally, the following table presents the remaining parameters from Falcon 9 that were used in the simulation:

Parameter	First Stage	Second Stage
Isp (Sea Level)	283 s	–
Isp (Vacuum)	312 s	348 s
Maximum Thrust (SL)	7,607 kN	8,227 kN
Maximum Thrust (V)	–	981 kN
Propellant	LOX/RP-1	LOX/RP-1
Propellant Mass	395,700 kg	92,670 kg
Empty Mass	25,600 kg	3,900 kg
Payload Capacity (LEO)	–	22,800 kg
Payload Capacity (GTO)	–	8,300 kg
Diameter	3.7 m	3.7 m

Table 2: Falcon 9 block 5 Parameters [14] [15] [16]

4.2.2. Simulation Parameters

The time steps for the integration of the rocket dynamics are set to 0.001 s to ensure high resolution and accuracy of the results. The pitch maneuver is simulated to start after 7.5 s after lift off and the duration of it was rounded down to 45 s.

The optimization is done with respect to a typical desired circular Low Earth Orbit with an altitude of 500 km, matching Starlink satellites' orbit height [17]. To ensure that the optimizer does not have any problems with convergence and gives wrong results, the brute-force optimizer is used. The tested range of steering angles is $[0.001°; 6°]$. Pre-simulations have shown that higher values do not result in feasible scenarios. The number of tested angles of the brute-force optimizer is set to 2000, leading to a resolution of about 0.003°.

4.3. Results

In Fig. 3 and Fig. 4, the results of the optimal found trajectory for a desired orbit of 500 km are depicted. It has to be noted that the timeline of the plots of the CDB approach stops before the second Δv_2 is applied. This is done to enable an analysis of the results until the first Δv_1 and to compare them with the CSB approach. The plots for the gravity, drag and total loss over time are given in Fig. 6. The according visualization is shown in Fig. 5. The detailed results for all three tested altitudes are given in Tab. A.3 and A.4 in the Appendix A.

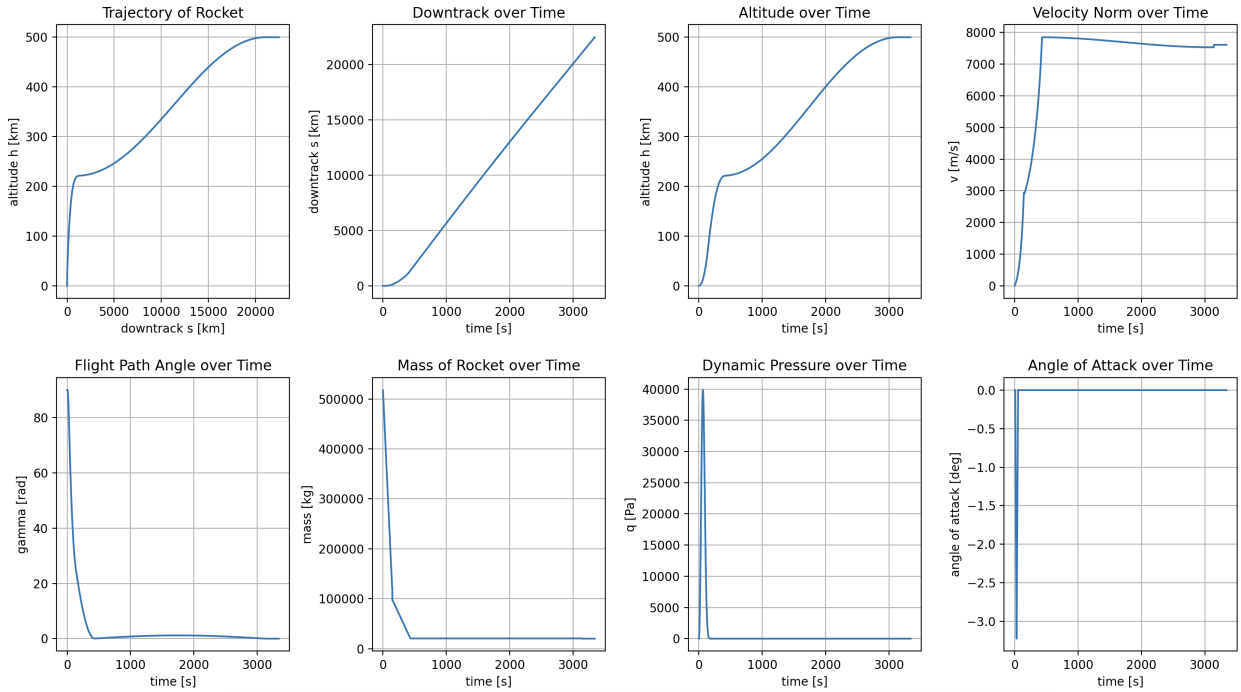

Figure 3: Plot of the results over time for the CSB simulation for the desired orbit of 500 km.

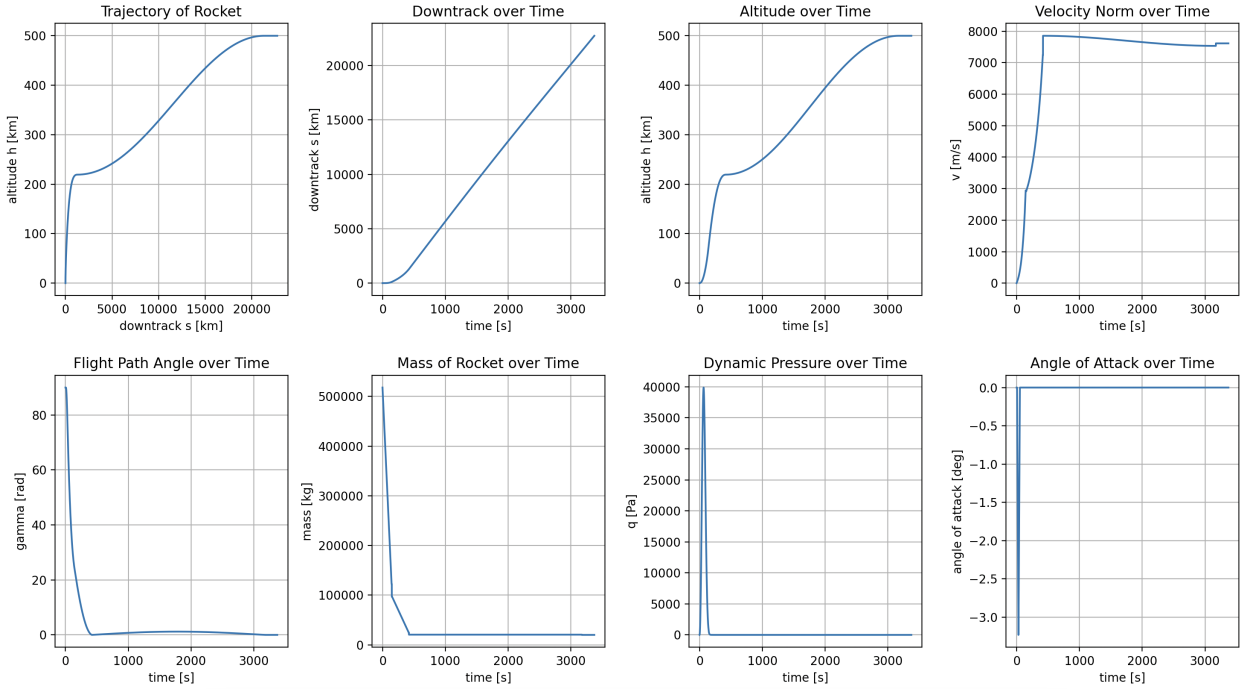

Figure 4: Plot of the results over time for the CDB simulation for desired orbit of 500 km.

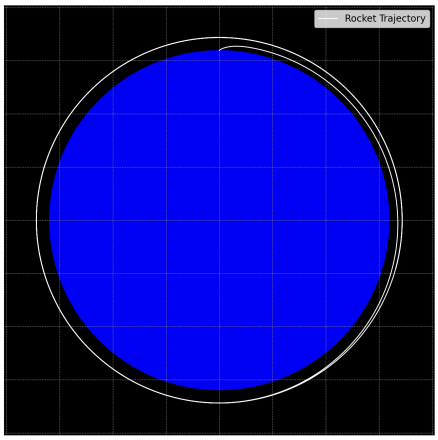

(a) CSB

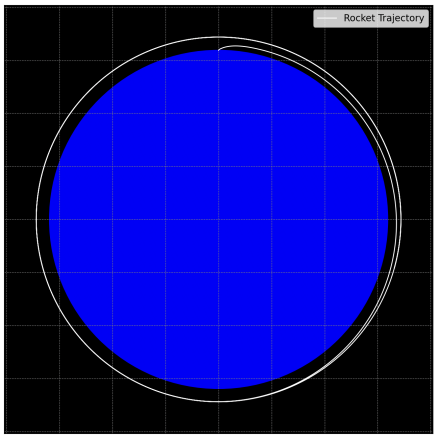

(b) CDB

Figure 5: Trajectory visualization for desired orbit of 500 km for single (CSB) and double burn (CDB) simulations.

4.4. Discussion

The CSB rocket flight starts with the lift-off in the thrust phase where $\gamma = 90°$ (see "Flight Path Angle over Time" graph of Fig. 3) and 7.5 s later the pitch maneuver begins with an initial kick angle, returning the angle of attack to zero shortly after ("Angle of Attack over Time" graph of Fig. 3). Hence, the rocket rapidly gains altitude to escape from the atmospheric/gravity effects as soon as possible while increasing velocity ("Velocity Norm over Time" graph of Fig. 3) with the help of the gravity-turn, leading to *Max Q* ("Dynamic Pressure over Time" graph of Fig. 3). At the same time that the mass decreases as a result of the propellant burning (see "Mass of Rocket over Time" graph of Fig. 3), it can be seen from the "Altitude over Time" representation of Fig. 3 that the main contribution in the displacement during this phase takes place in the vertical axis. Meanwhile, the flight path angle keeps increasing smoothly. Following, the first engine shuts down (MECO) at approximately 70 km of altitude and is separated, followed by the second engine ignition. Behavior that the "Velocity Norm over Time" graph of Fig. 3 reveals because of a discontinuity in the

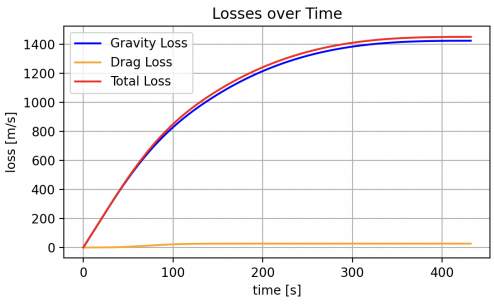

(a) CSB

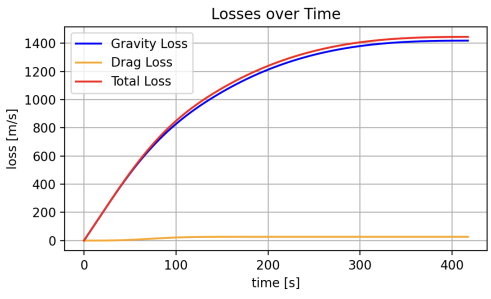

(b) CDB

Figure 6: Plot of the gravity, drag and total loss over time for desired orbit of 500 km for single (CSB) and double burn (CDB) simulations.

velocity at around 160 s after the lift-off and can be verified with the "Mass of Rocket over Time" Fig. 3 since the mass of the rocket decreases linearly up to that specific moment. Then, the effect of the gravity-turn takes a more relevant role by making the derivative of the downtrack with respect to time larger than the respective one from altitude, leading to an increase in the velocity until it reaches its maximum value at 221 km of altitude (see Appendix A). At this instant, the flight path angle, γ, becomes 0, which produces the beginning of the coasting phase and atmospheric effects can be assumed negligible, meaning the rocket has arrived at the apogee of the trajectory around Earth. Therefore, the engine cut-off occurs and the velocity decreases as a result, stopping the reduction in the mass of the rocket. Afterwards, a small deviation in γ from 0° can be spotted as the orbit after coasting started is elliptical. An engine ignition after 3000 s is performed to provide the necessary Δv to get to the desired circular orbit at 500 km of altitude.

Regarding the CDB rocket flight, it can be seen that results are very close to the previously stated, which reveals that the optimal strategy would be CSB, since the double burn scenario always tries to approach it by doing a high first burn and a small second one (no differences are seen in the scale of Fig. 5 neither in the Tab. A.3 or A.4). This behavior is corroborated by the fact that it is repeated for all tested altitudes.

4.4.1. Payload Mass

The payload capacity that emerged from the simulation is quite lower than the true Falcon 9 capacity. For example, for LEO orbit, it is 70% less than what Falcon 9 can provide (22 800 kg [14]). This happens because the trajectory employed by SpaceX is better optimized than the gravity turn simulated. Furthermore, it is important to state that, for this project, the value of C_D has been assumed to be constant when, in reality, it depends on the velocity and on the changing atmosphere when altitude increases. Additionally, the value of 0.3 chosen, the average of the data from Saturn V rocket [13], may be larger than the one Falcon 9 would have due to the significant differences in the shape.

4.4.2. Max Q

As previously addressed, dynamic pressure during flight increases until it reaches a so-called Max Q value, point where mechanical stress on the rocket peaks due to a combination of the velocity of the rocket and resistance created by the atmosphere of the Earth [18]. The exact value of Max Q for the Falcon 9 can vary depending on the mission profile, payload, and ascent trajectory, as can be proved with the results contained in the Appendix A. However, as mentioned earlier, the Max Q during ascent typically falls within the range of 14–23 kPa, fact that contrasts with the results of the simulation. Falcon 9 uses Merlin engines, which are capable of throttling down to approximately 60% of full thrust [11]. Evidence from simulations and analyses supports that thrust is reduced to keep dynamic pressure around 25 kPa, then gradually increased post-Max Q, diminishing the peak dynamic pressure and protecting the vehicle's structure. This is the reason why real values differ from the 39 kPa obtained in the simulations where maximum trust was considered.

4.4.3. Δv and Losses

For the 500 km scenario only, using Tsiolkovski's equation, the following total ideal Δvs can be obtained:

- $\Delta v_{CSB} = 9.378\,\mathrm{km\,s^{-1}}$
- $\Delta v_{CDB} = 9.375\,\mathrm{km\,s^{-1}}$

These values can be compared with Falcon 9's, whose Δv, using Tsiolkovski's equation with the data from [11] (assuming maximum payload configuration), corresponds to $8.767\,\mathrm{km\,s^{-1}}$. Considering that Falcon 9's trajectory is more optimized and that the considered data might not exactly refer to the simulated conditions, the value obtained through the simulation can therefore be considered sufficiently close to the real one.

The actual orbital speed can be obtained from the following relationship [2]:

$$\Delta v_{actual} = \Delta v_{ideal} - \Delta v_{drag} - \Delta v_{grav} = \Delta v_{ideal} - \Delta v_{losses} \tag{15}$$

where values of Δv_{losses} for both injection strategies are obtained from Tab. A.3 and A.4.

The evolution of losses due to drag and gravity can be seen in Fig. 6a and 6b. Even though data from Falcon 9 is not publicly available to verify the obtained results, the evolution of both graphs is as expected: the cumulative drag losses increase during the first phases of the launch and then remain constant, while the cumulative gravity losses keep increasing in a monotonous way, reaching a stationary point in correspondence with the injection into a circular orbit (no further increase in altitude).

5. Other Approaches

5.1. Two-Point Boundary-Value Problem

Aside from the optimization method considered in this report, other approaches to solve this problem do exist. While the lift-off and coasting phases are described by the same equations, the latter is usually optimized in a different way; using indirect methods, the problem can be transformed into a Two-Point Boundary-Value Problem (TPBVP) and solved using a Hamiltonian function and applying Pontryagin's Minimum Principle [19].

There are three different methods (used to solve the Single-Point Boundary-Value Problem) which, when combined in pairs, allow for the solution of the TPBVP [20]:

1. Direct expansion of the coordinates as Taylor series of time [20];
2. Use of the atmospheric mass density as an altitude variable and explicit it as a function of the remaining propellant mass fraction [20];
3. Use the inverse of the atmospheric mass density as altitude variable and explicit it as a function of the burned propellant mass fraction [20].

When combining the first and third methods, it is possible to find out whether the solution exists and if the rocket has sufficient performance to reach the final conditions; if it does, it then allows for the calculation of the trajectory and the performance envelope of the rocket [20]. Both the combinations of the first and second methods, and of the second and third methods do not return a feasible solution [20], suggesting that method 2 cannot be used to solve the TPBVP, but only the Single-Point Boundary-Value Problem [20].

5.2. Launch Example

This section comprises an analysis of a real Falcon 9 mission launch drawing on publicly available timelines and mission reports (e.g., SpaceX CRS missions and Transporter-1 [12] [21]) that details the key flight phases and control maneuvers used in practice.

The Falcon 9 lifts off from the launch pad powered by its nine Merlin engines and immediately after liftoff, the vehicle climbs vertically. As previously stated, this is essential to minimize aerodynamic drag and gravity losses while the rocket is still close to the pad.

However, almost as soon as the rocket clears the tower, typically around $T + 7$ to $T + 10$ seconds, the onboard guidance system commands a slight pitch maneuver (pitchover) which is a very small angular change (often just a few degrees) that begins the gravity turn. In this phase, engine gimballing and pre-programmed pitch schedules reorient the vehicle so that its trajectory gradually transitions from vertical to one that builds horizontal speed. This early turn is critical because as gravity begins pulling on the vehicle's velocity vector, the rocket naturally falls into a curved trajectory that minimizes gravity losses.

At $T + 70$ seconds, the rocket reaches supersonic speed, and shortly thereafter, it passes the area of maximum dynamic pressure (Max Q). To protect the structure, the engines are throttled down slightly during this period.

After the vehicle has accelerated substantially, around $T + 158$ seconds, the first-stage engines are shut down at MECO. By this point, Falcon 9 has reached an altitude of roughly 80 km and is travelling at Mach 10. Just a few seconds later, the first stage separates from the second stage. This separation is executed with precise timing to ensure minimal disturbance to the remaining stage's trajectory. Immediately after separation, the single Merlin Vacuum engine on the second stage ignites (typically within 5–8 seconds after MECO). Almost simultaneously or shortly thereafter (around $T + 2$ minutes 50 seconds), the payload fairing is jettisoned once the rocket has climbed above the thickest portion of the atmosphere. This removal reduces mass and aerodynamic drag, allowing the second stage to accelerate more efficiently.

Then, the second stage performs a sustained burn lasting roughly 6–7 minutes to raise the payload. Depending on the mission profile, the second stage may coast briefly and then execute a final burn (or burns) to circularize the orbit. For example, in many CRS missions, after a first engine cutoff (SECO) the payload begins its autonomous orbital operations.

In missions where booster recovery is planned, after stage separation the first stage reorients using grid fins and initiates a boostback burn to reverse its downrange momentum. This is followed by an entry burn as it reenters the atmosphere, and finally a landing burn that slows the stage for a vertical touchdown on a drone ship or ground pad, typically landing around $T + 9$ minutes. While the recovery sequence is independent of the payload trajectory, its timing is coordinated so that the first stage can safely return without affecting the ascent.

Following second-stage cutoff, payload-specific events occur. For instance, in a Dragon mission the spacecraft separates from the second stage and autonomously deploys solar arrays and initiates communication with the ISS. In rideshare missions like Transporter-1, multiple small satellites are sequentially deployed according to a preplanned timeline.

6. Conclusion

The goal of this project was to analyze two gravity-based launch approaches, namely CSB and CDB, and develop a simulation that optimizes the steering angle during the pitch maneuver to minimize the required propellant. This report will be concluded by stating out the most important findings of this project.

First, as it was seen in the theoretical considerations (Sec. 2.4), a rocket cannot get into any desired circular orbit by only using a "pure" gravity turn. It needs to adjust its velocity, e.g. by adding a coasting phase or by throttling the engines at some point to guarantee reaching the desired altitude with the correct speed.

Second, after analyzing both approaches for different altitudes, it was seen that the optimization of the CDB method always converges to a solution which is similar to the CSB approach. This may indicate that the CSB is the optimal strategy.

Third, it has been seen that both optimized gravity-turn based approaches result in less payload available to carry to LEO than by Falcon 9, even though similar rocket parameters are used. This difference results not only because of the constraints and necessary assumptions to simply the problem and the simulation but also due to the fact that much more advanced control techniques regarding the steering angle are applied to further optimize the trajectory in real-life.

Fourth, the simulation resulted in much higher values for the Max Q than expected when considering the Max Q of Falcon 9. This can mainly be reasoned because during the launch of Falcon 9, the main engine is throttled down to reduce the maximum dynamic pressure.

Fifth, the simulation showed that the influence of gravity losses on the trajectory is much larger than of the drag losses. Thus, it can be confirmed that it is optimal to start the pitch maneuver as soon as the launch tower was cleared in order to minimize them.

Last, talking about propellant, it was observed that the greater contribution to the consumption occurs until MECO phase (Sec. 4.4), verifying that the first stage represents the main part of the total propellant.

References

[1] U. Walter, Astronautics: The Physics of the Space Flight, 3rd Edition, Springer, 2008.

[2] Creig A. Kluever, Space Flight Dynamics, Wiley, 2018.

[3] G. R. . M. L. Ruggiero, Relativity in Rotating Frames, Kluwer Academic Publishers, 2004.

[4] A. D. Ogundele, Nonlinear dynamics and control of spacecraft relative motion, Nombre del Journal.

[5] D. Edberg, W. Costa, Design of Rockets and Space Launch Vehicles, 2nd Edition, American Institute of Aeronautics and Astronautics, Inc., 2022.

[6] Glenn Research Center, Dynamic pressure, https://www1.grc.nasa.gov/beginners-guide-to-aeronautics/dynamic-pressure-2/, accessed on 2025-3-25 (2024).

[7] SpaceX, Spacex youtube channel, https://www.youtube.com/@SpaceX, accessed: 2025-03-29 (2008).

[8] SpaceX, Crs-9 hosted webcast, https://www.youtube.com/watch?v=ThIdCuSsJh8, accessed: 2025-03-29 (2016).

[9] SpaceX, Jason-3 hosted webcast, https://www.youtube.com/watch?v=ivdKRJzl6y0, accessed: 2025-03-29 (2016).

[10] H. D. Curtis, Orbital mechanics for engineering students, Butterworth-Heinemann, 2019.

[11] SpaceX, Falcon user's guide, https://www.spaceflightnow.com/falcon9/001/f9guide.pdf, accessed on 2025-3-25 (2021).

[12] SpaceX, Spacex crs-6 mission press kit, https://www.nasa.gov/wp-content/uploads/2018/07/spacex_nasa_crs-6_presskit-2.pdf, accessed: 2025-03-29 (2015).

[13] M. Sagliano, Apollo 11 reloaded: Optimization-based trajectory reconstruction, in: AIAA Scitech 2021 Forum, 2021, p. 1344.

[14] SpaceX, Falcon 9, https://www.spacex.com/vehicles/falcon-9/, accessed on 2025-3-25 (2025).

[15] NASA, Space launch report: Spacex falcon 9 v1.2 data sheet, https://sma.nasa.gov/LaunchVehicle/assets/spacex-falcon-9-v1.2-data-sheet.pdf, accessed on 2025-3-27 (2018).

[16] wevolver, Falcon 9 v1.2 or full thrust - block 5, https://www.wevolver.com/specs/falcon-9-v12-or-full-thrust-block-5, accessed on 2025-3-27 (2019).

[17] Starlink, How starlink works, https://www.starlink.com/technology, accessed on 2025-3-23 (2025).

[18] AmericaSpace, Static fire test of the falcon 9 core in preparation for nrol-76 launch, https://www.americaspace.com/launchsequencer.php?Launch=205&utm_source=chatgpt.com, accessed: 2025-03-29 (2017).

[19] Morgado, F. Marta, Andre Gil, Paulo., (2022) Multistage rocket preliminary design and trajectory optimization using a multidisciplinary approach. , Structural and Multidisciplinary Optimization. 65. doi:65.10.1007/s00158-022-03285-y.

[20] M. B. C. Campos, L., Gil, P. J. S., (2020) The Two-Point Boundary-Value Problem for Rocket Trajectories., Aerospace, 7(9), 131. doi:https://doi.org/10.3390/aerospace7090131.

[21] Falcon 9 launch timeline on the Transporter-1 mission – Spaceflight Now, https://spaceflightnow.com/2021/01/23/falcon-9-launch-timeline-on-the-transporter-1-mission, [Online; accessed 31. Mar. 2025] (Mar. 2025).

[22] R. Storn, K. Price, Differential evolution–a simple and efficient heuristic for global optimization over continuous spaces, Journal of global optimization 11 (1997) 341–359.

A. Detailed Results

Parameter	**500 km**	**2000 km**	**20000 km**
Optimal Kick Angle (deg)	-3.23	-3.23	-3.23
Optimal Altitude to Stop Burning (km)	221.58	221.66	222.82
Optimal Time to Stop Burning (s)	431.86	439.53	464.83
Optimal Δv (m/s)	79.06	422.39	1427.78
Propellant Overview (2nd Stage)			
Propellant Left (kg)	16611.97	14512.45	7590.65
Propellant Used (kg)	76058.03	78157.55	85079.35
Propellant for Circularization (kg)	469.58	2142.81	3927.37
Total Propellant Used (kg)	76527.61	80300.36	89006.72
Possible Payload (kg)	16142.39	12369.64	3663.28
Burn Time for Δv (s)	1.72	7.83	14.35
Final Orbital Elements			
Semi-Major Axis (m)	6877917.96	8377801.67	26374078.05
Eccentricity	5.96×10^{-6}	1.18×10^{-5}	7.43×10^{-5}
Apoapsis Altitude (km)	499.96	1999.90	19998.04
Periapsis Altitude (km)	499.88	1999.70	19994.12
Maximum Dynamic Pressure (Pa)	39841.73	39841.73	39841.73
Losses			
Gravity Loss (m/s)	1424.22	1424.31	1425.46
Drag Loss (m/s)	26.64	26.64	26.64
Total Loss (m/s)	1450.86	1450.95	1452.10

Table A.3: Simulation Results for Different Altitudes in CSB scenario

Parameter	**500 km**	**2000 km**	**20000 km**
Optimal Kick Angle (deg)	-3.23	-3.23	-3.18
Optimal Altitude to Stop Burning (km)	219.36	220.23	238.70
Optimal Time to Stop Burning (s)	417.15	425.15	464.96
Optimal Δv_{total} (m/s)	688.58	1082.46	1426.68
Optimal Δv_1 (m/s)	608.90	659.65	1426.24
Optimal Δv_2 (m/s)	79.69	422.81	0.43
Propellant Overview (2nd Stage)			
Propellant Left (kg)	20642.10	18450.77	7519.59
Propellant Used (kg)	72027.90	74219.23	85150.41
Propellant for Circularization (kg)	4482.88	6073.27	3900.65
Total Propellant Used (kg)	76510.78	80292.50	89051.06
Possible Payload (kg)	16159.22	12377.50	3618.94
Burn Time for Δv_1 (s)	14.65	14.35	14.25
Burn Time for Δv_2 (s)	1.73	7.84	0.0035
Final Orbital Elements			
Semi-Major Axis (m)	6878034.63	8378051.99	26378904.08
Eccentricity	4.93×10^{-6}	5.37×10^{-6}	5.56×10^{-6}
Apoapsis Altitude (km)	500.07	2000.10	20001.05
Periapsis Altitude (km)	500.00	2000.01	20000.76
Maximum Dynamic Pressure (Pa)	39884.58	39867.15	39592.75
Losses			
Gravity Loss (m/s)	1418.68	1420.90	1461.19
Drag Loss (m/s)	26.72	26.68	26.20
Total Loss (m/s)	1445.40	1447.59	1487.39

Table A.4: Simulation Results for Different Altitudes in CDB scenario

B. Software Program

This section gives a brief summary of the developed software "Simulation of a Two Stage Rocket Launch Performing a Gravity-Turn with Atmosphere", version 1.0.0 (first official release, 30.3.2025). The software implements simulation for a gravity-turn based ascent trajectory of a two-stage space rocket. Two different trajectory types are implemented as presented in this work 2.5: Coasting Single Burn (CSB) and Coasting Double Burn (CDB).

The software optimizes the maximum angle of attack during the pitch maneuver with respect to the used propellant of the second stage to maximize the payload the launcher could

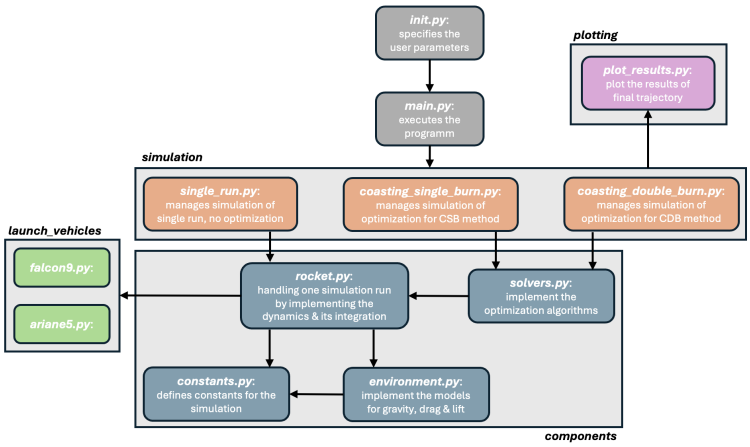

Figure B.7: Block diagram of the software architecture. Arrows indicate the interaction between files (file of start of arrow calls file of end of arrow). Grey boxes indicate the files lie in the same folder and belong to the same sup-group.

bring to the desired orbit. A detailed description of the software is given in section 3 where all inputs and outputs are explained. A block diagram showing the software architecture is given in Fig. B.7.

The software was developed and tested in *Python 3.9.13*. The following python packages were used for implementing the simulation: *numpy* (version 2.0.2), *scipy* (version 1.13.1) and *matplotlib* (version 3.9.4). Within the simulation, two major external algorithms are used. First, for integrating the differential equations of motion, the *integrate.solve_ivp()* function of the *scipy* package is used which implements the the Runge-Kutta 5 algorithm. Second, *scipy*'s *optimize.differential_evolution()* and *optimize.brute()* function is integrated which implements the differential evolution [22] and a brute-force method respectively for optimization purposes.

The software is published over `https://github.com/JoshRedelbach/gravity_turn`. There, a user-guide is provided. In general, the software can simply be executed by specifying the desired parameters in the *init.py*-file and by running the *main.py*-file

C. Contributions

Name	Contribution	Qualitative Evaluation
Rodrigo Pereira	Sec. 2.8, 4., 5.2, Research	100%
David Ribeiro	Sec. 2.2, 2.6, 2.7, 4., 6.	100%
Alexandre Pereira	Sec. 3., SW	100%
Alessandro Melifiori	Abstract, Sec. 1., 2.1, 2.3, 4., 5.1	100%
Marta Pellegrino	Abstract, Sec. 1., 2.1, 2.3, 4., 5.1	100%
João Almeida	Sec. 2.8, 4., 5.2, Research	100%
Joshua Redelbach	Sec. 2.4, 2.5, 3., App. A, App. B, SW	100%